CHALMERS

Microwave Technology for Detection of Traumatic Pneumothorax: Development of a Wearable Microwave Antenna Array and Evaluation on Thoracic Phantom

Master's Thesis in Biomedical Engineering

Robert Samo & Prateek Saraswat

Department of Signals Systems
Chalmers University of Technology
Gothenburg, Sweden, September 2013
Master's Thesis: EX034/2013

Abstract

Traumatic injuries cause approximately 27.3 deaths per 100,000 population per year in the USA and 10 deaths per 100,000 population per year in the EU.In Nordic countries, however, this rate is much higher at a median value of 44.8 deaths per 100,000 population per year. A quarter of all deaths caused by traumatic injuries are a consequence of trauma to the thorax. A pneumothorax (PTX), an accumulation of air in the intrapleural space, is a common, potentially life-threatening traumatic thoracic injury. If left untreated, a growing PTX can lead to a complete cardiovascular collapse and ultimately death. Therefore it is important to diagnose a PTX early, preferably in a prehospital setting. The diagnosis is presently made primarily through physical examinations. However physical examinations require a high level of operator competency, and may not be feasible in presence of ambient noise. Microwave technology has shown to be promising for detecting traumatic brain injury. The aim of this thesis was to develop a wearable microwave antenna array and investigate the potential of microwave technology to detect a PTX simulated in a thoracic phantom.

The novel wearable microwave antenna array was constructed using six in-house fabricated patch antennas incorporated into a leather belt. A thoracic phantom was constructed using plastic containers of sizes corresponding to the physical dimensions of the thorax; filled with appropriate mixtures of ethanol and deionised water, to obtain realistic dielectric properties. A container in the shape of an elliptical frustum represented the thorax cavity, two cylindrical containers formed the lung space, and balloons placed inside the lung space simulated collapsed lungs. In this way, a healthy individual, and PTX of different sizes (50%, 20% and 10%) were modelled in phantoms. For each phantom 3×10 measurements were made in a random fashion. The belt was repositioned after every third measurement to incorporate variability in the position of the belt. Measurements were also made on a PTX of progressively decreasing size. Data gathered from these phantoms were analysed using a classification algorithm based on singular value decomposition.

Results of analysing the data gathered from the various phantoms indicated that a PTX can be detected using the proposed microwave technique, even in the presence of variability in the belt position. Through an analysis of data collected on a progressively decreasing PTX, it was shown that changes in the net dielectric properties of the phantom, caused by the presence of intrapleural air were detectable. This technology demonstrates promising results for objective detection of a PTX and monitoring its progression; it has the potential to be developed into a system that can be deployed in ambulances. But during tests it was seen that the results can be affected by factors like instrument calibration, and the days on which the measurements were made. Also the phantom used only provides a static test environment: one that does not change in any way during the course of a single measurement instance. To continue development, the phantom can be further improved. Animal studies could be made to provide useful insights on how the wearable instrument will perform on living subjects.

Abstract

Traumatiska skador orsakar cirka 27.3 dödsfall per 100.000 invånare årligen i USA och cirka 10 dödsfall per 100.000 invånare årligen i EU. I nordiska länder är dock siffran mycket högre, då det årligen sker cirka 44.8 dödsfall per 100.000 invånare. En fjärdedel av alla dödsfall orsakade av traumatiska skador är en konsekvens av thoraxtrauma. Pneumothorax (PTX), en samling av luft i det intrapleurala utrymmet, är en potentiellt livshotande traumatisk thoraxskada. Om PTX förblir obehandlad, kan en växande PTX leda till en komplett kardiovaskulär kollaps och slutligen död. Därför är det viktigt att diagnostisera PTX tidigt, fördelaktigast i en prehospital miljö. I dagsläget utförs diagnosen genom fysiska undersökningar. Dock kräver dessa fysiska undersökningar en hög nivå av operatörskompetens och är möjligtvis inte fördelaktiga vid förekomst av omgivande ljud. Mikrovågsteknik har visats sig vara en lovande teknik för detektion traumatiska hjärnskador. Målet med detta examensarbete är att utveckla en uppställning av mikrovågsantenner som kan bäras utav patienter och undersöka mikrovågsteknikens potential att detektera PTX, simulerad i en thoraxfantom.

Den nya bärbara uppställningen av mikrovågsantenner var konstruerad med sex antenner som var bundna till ett läderbälte. En thoraxfantom var konstruerad med plastbehållare, av lämpliga dimensioner, som fylldes med lösningar, bestående av etanol och destillerat vatten, för att erhålla realistiska dielektriska egenskaper. En behållare formad som en elliptisk stympad cylinder representerade thoraxhålan, två cylindrar representerade lungutrymmet och ballonger användes, placerade inuti lungutrymmet, för att simulera kollapsade lungor. Med denna uppsättning modellerades fantomer med PTX av olika storlekar (50%, 20% och 10%), samt en fantom som representerade en frisk individ. För varje fantom gjordes 3×10 mätningar i slumpmässig ordning. Bältet flyttades till en ny position efter var tredje mätning för att inkorporera variabilitet i bältets position. Mätningar gjordes också på en progressivt minskande PTX. Samlad data från samtliga fantomer analyserades med hjälp utav en klassificeringsalgoritm baserad på singulärvärdesuppdelning.

Resultat från analys av data, samlad från en fantom som representerar en frisk individ och fantomer som representerar PTX av olika storlekar, indikerar att PTX kan detekteras med den föreslagna mikrovågstekniken, trots variation i bältets position. Analys av data samlad från en fantom med en progressivt ökande PTX, visar att förändringar i fantomens dielektriska egenskaper, på grund av förekomst av luft, kunde detekteras. Dessa resultat indikerar att denna teknik är lovande för objektiv detektering av PTX, och har potentialen att vidare utvecklas till ett system för användning i ambulansmiljö. Resultaten är också lovande för att monitorera förloppet av en PTX. För fortsatt utveckling, kan fantomens anatomiska och geometriska egenskaper ytterligare förbättras. Djurstudier kan utföras för att ge insikt över hur det bärbara instrumentet presterar på en levande individ. Det förekommer en stor oönskad variabilitet i samlad mätdata på grund av ändringar i mätuppställning och mätinställningar, vilket måste hanteras i framtiden.

Acknowledgements

Good work is rarely done in complete isolation. There have been many people who, in their own way, have contributed to this thesis. We would like to acknowledge their contributions and express our gratitude for their support. We like to thank our supervisor Stefan Candefjord, and our examiner Andreas Fhagher, for their guidance and support. We would like to thank Hana Trefna from the Signals and System department at Chalmers for helping us in familiarising ourselves with the measurement equipment, and for designing the antennas that were used. Stefan Kidborg from Medfield Diagnostics gave us valuable advise on phantom construction, and to him we also express our thanks. And last, but certainly not the least, we express our gratitude to Tomas McKelvey and Yinan Yu, for providing the classifier which was used in the data analysis.

Prateek and Robert, Gothenburg (September 09, 2013)

Contents

List of Figures

List of Tables

List of Abbreviations

°C Degrees celcius

AP Anterior posterior

CA California

cm centimetre

CT Computed tomography

dB Decibel

ECal Electronic calibration module

EU European Union

F/m Farad per metre

GHz Giga Hertz

HIV Human immunodeficiency virus

Hz Hertz

ICH Intra-cranial hemorrhage

IPP Intra-pleural pressure

kg Kilo gram

m metre

MHz Mega Hertz

ml millilitre

MWH Microwave helmet

PNA Programmable network analyser

PTX Pneumothorax

S/m Siemens per metre

US United States of America

1

Introduction

TRAUMATIC injuries cause approximately 27.3 deaths per 100,000 population per year in the USA, and 10 deaths per 100,000 population per year in the EU[1, 2]. For Nordic countries (Finland, Denmark, Norway and Sweden) this number is higher, at a median value of 44.8 deaths per 100,000 population per year[3]. For comparison, the number of deaths due to cancer in the US was 567.614 people in 2009[4], which works out to be around 0.19 deaths per 100,000 population, in that year. A quarter of the deaths due to trauma are a consequence of injuries to the thorax (chest); two thirds of the deaths resulting from thorax trauma occur after the victim has reached the hospital[5]. A pneumothorax (PTX), a collection of air in the thoracic cavity[1] caused by a rupture in the lung, and a hemothorax, a collection of blood in the thoracic cavity due to a rupture in the thoracic organs, are the two most common types of injuries found in victims of thoracic trauma[6]; these injuries often occur together[7]. Often a small, undetected PTX can rapidly progress to a tension PTX; a situation where injury to the lung results in a 'one-way valve' being created, so air leaks out from the lung into the pleural space[2] but is unable to escape from it[5]. This results in a progressive increase in intra-pleural pressure[3] to the point where it starts interfering with venous return by causing blood pooling in capacitance vessels of the lung[4], which causes severe dyspnea (difficult or laboured breathing) and can lead to cardiovascular collapse. This makes early detection important, particularly in patients receiving mechanical ventilation, where the diagnosis of a PTX can influence ongoing assessment and management[7].

[1]The thoracic cavity is the space in the human body enclosed by the ribs, breastbone, spinal column, and diaphragm.

[2]The pleural space is the space between the inner (visceral) and outer (parietal) pleura (the double layered membrane around the lungs)[8]

[3]Intra-pleural pressure (IPP), is the pressure inside the pleura. IPP needs to be negative to keep the lung inflated.

[4]The Capacitance vessels are the blood vessels in the chest region, that hold the majority of the intra-vascular blood volume.

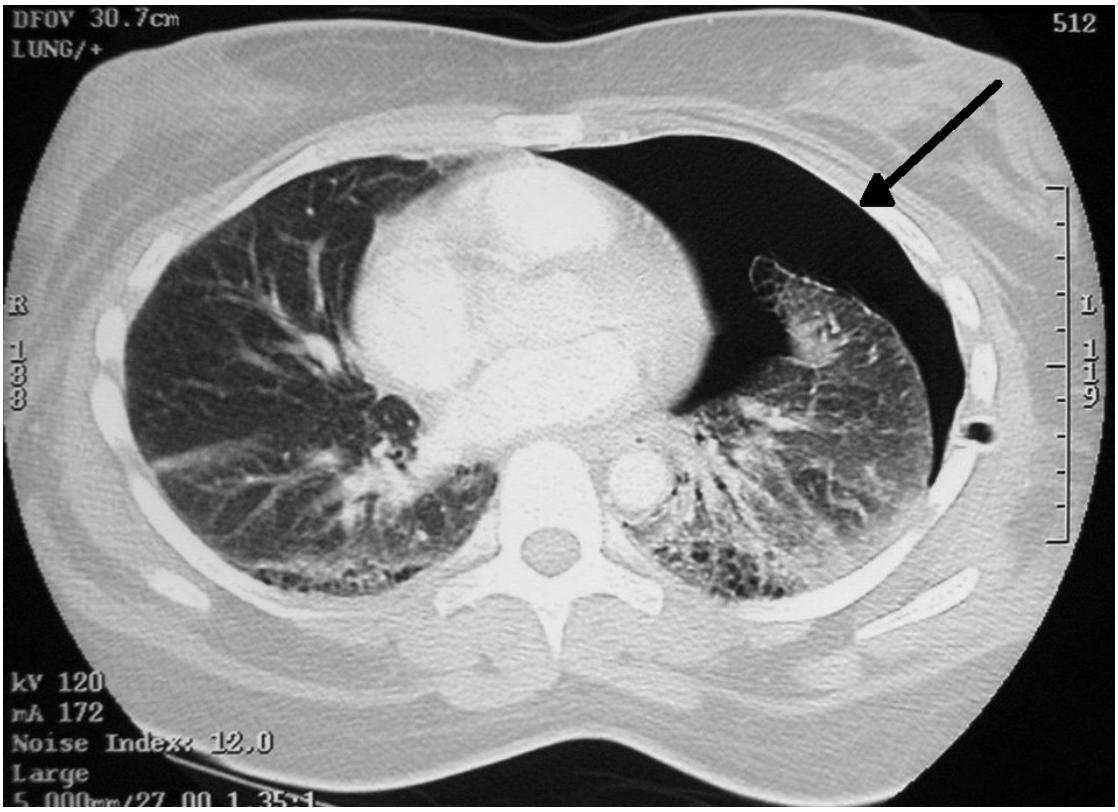

Figure 1.1: A CT scan of the human thorax with a pneumothorax (PTX) present in the right lung (Source:Clinical Cases, Pneumothorax CT (2006): `http://en.wikipedia.org/wiki/File:Pneumothorax_CT.jpg`).

Since a hemothorax often accompanies a traumatic PTX, it becomes essential to study these injuries together. Figure 1.1 shows a computed tomography (CT) scan, in the axial plane, of a human thorax with a PTX present in the right lung.

In the hospital setting a PTX may be diagnosed through a supine anterior-posterior chest X-ray examination (AP X-ray), physical examinations (which involve listening to lung sounds, blood gas analysis, and monitoring the patients blood pressure), ultrasound, and CT scans[9]. CT is currently the gold standard for the detection of PTX while an AP X-ray or a physical examination are the most widely used primary diagnosis modalities[5, 10]. Similar to a PTX, the diagnosis of a hemothorax involves AP thorax X-rays or a physical examination of the patient, and CT is the gold standard for detection[11].

Retrospective studies on thoracic trauma have shown that in approximately half of the cases, a PTX was not initially suspected in an AP chest X-ray or physical examinations but was later detected through CT scans; this type of PTX is referred to as an

occult PTX[7, 12]. If a successful diagnosis of a PTX can be made early, the patient may receive appropriate treatment faster; administering the right treatment can have a positive affect on patient survivability[13]. In an ambulance, an X-ray machine is not available, and detecting a PTX through physical examinations can prove difficult in the presence of ambient noise, e.g. during air transports[9]. Diagnosing a PTX only through physical examination also requires a high level of operator competency and the results may be subjective with a strong possibility of missing an occult injury[7].

There is therefore a need to develop a new diagnostic tool, for objective detection of chest injury. One that is fast, portable, and accurate, for the a detection of a PTX and hemothorax; either at the scene of th accident or during transportation to a medical facility. A system where the measurement procedure is simple and measurement results are not subjective to operator interpretation. A prerequisite to designing an effective diagnosis modality is to have a good understanding of the nature of the injury or ailment that is to be detected.

1.1 Pneumothorax

A PTX is a collection of air in the pleural space. Because of this collection of air, the negative pressure in intra-pleural space, which is needed for the lung to maintain its patency[5], is lost and the lung collapses. A PTX is a common result of traumatic thoracic injury[6] or disease, and it may even occur spontaneously[5]. In the specific case of preterm neonates, a PTX may also occur due to bursting of alveoli caused by an excess pressure exerted by a mechanical ventilator, which causes air to leak out of the lungs. This air leak, combined with the inability of newborns to produce enough surfactant proteins (which increase the cohesion and adhesion properties of the pleural fluid) in the pleural fluid, may cause the lung to collapse[14]. Certain medical procedures are also associated with inducing a PTX and because the presence or absence of a PTX may direct the ultimate course of treatment; a high degree of suspicion for development of a PTX is advised in all cases of mechanical ventilation where the patient exhibits shortness of breath[5].

A PTX is clinically classified as either traumatic or spontaneous, depending on its cause. A traumatic PTX can also be classified into an non-iatrogenic (resulting from injury) or an iatrogenic (resulting from medical treatment) PTX[10]. A spontaneous PTX is further classified into a primary, secondary or catamenial PTX[10].

1.1.1 Traumatic pneumothorax

A non-iatrogenic traumatic PTX is the most common consequence of chest trauma, after rib fractures, and can be observed in 40–50% of cases of patients with chest trauma[13]. A traumatic PTX may also be a result of blunt trauma to the abdomen[15]. In the

[5]Patency is the condition of being open, expanded, or unobstructed.

case of trauma patients in general, (chest trauma and otherwise) studies have shown that about 50% have an occult PTX[13]. Thus it is important to have a high suspicion for a PTX during examination of multiple trauma patients and incorporate chest CT even if there is no obvious chest trauma. Furthermore, the importance of detecting a PTX in trauma patients who need medical ventilation is crucial, as medical ventilation may worsen an already existing PTX. In 20% of traumatic PTX cases there is also a hemothorax[13].

A traumatic PTX can be managed and treated by various methods; the size of the PTX is usually the determining factor for the treatment administered. In the case of a small sized PTX, the patient is just held under observation while being supplemented with oxygen; no treatment is required but the patient has to return for follow ups. In the case of a full PTX, the pleural space must be drained with a chest tube[10]. Studies report a low failure rate of 7–9% in traumatic non-occult PTX cases where chest insertion was not performed, and the patient was treated only through oxygen supplementation. Studies conducted on a large patient base have indicated that the size requirement for a PTX to require chest tube insertion is a margin of air greater than 1.5 cm (distance from the top of the chest to the injured lung), as seen in an AP X-ray[13].

An iatrogenic PTX is a result of surgical intervention or medical treatment. The complications of an iatrogenic PTX are significant, despite the strides in diagnostic techniques and increased use of invasive procedures. These complications may result in significant time delays in treatment, prolonged hospitalisation, morbidity, and even mortality[13]. An iatrogenic PTX may occur even if the clinicians are working in areas remote from the chest or respiratory tract. Thus it is recommended for clinicians to always maintain a high degree of suspicion for the risk of an iatrogenic PTX[13]. The most common causes of a iatrogenic PTX are presented in Table 1.1.

Table 1.1: The most common causes of iatrogenic PTX.[13]

Cause	%
Transthoracic needle lung biopsy	24
Subclavian vein catheterization	22
Thoracentesis	20
Transbronchial lung biopsy	10
Pleural biopsy	8
Positive pressure ventilation	7

1.1.2 Spontaneous pneumothorax

A PTX may occur spontaneously due to several reasons. A situation where a spontaneous PTX is the only present condition is called a primary spontaneous PTX (PSP)[10]. A PSP occurs in 7.4–18 cases in males and 1.2–6 cases in females per 100,000 population per year. These numbers are small compared to the incidences of traumatic injuries and injuries of this kind are not life threatening, although they can be discomforting to the patient[10]. Males, and subjects that are both tall and thin have a higher chance of developing a PSP, furthermore smoking also increase the risk of a PSP[10]. The causes of a spontaneous PTX are varied and not completely understood[5]. It is commonly believed that the pathogenesis of PSP is a spontaneous rapture of a air gap under the pleura[10, 16]. Spontaneous PTX treatment follows the same general guidelines as traumatic PTX, i.e. the size of the PTX determines if chest tube insertion to the pleural space is required.

1.2 Hemothorax

A Hemothorax is a collection of blood in the pleural cavity. For chest trauma hemothorax will often accompany a PTX. Blood may accumulate within the pleura as direct consequence of blunt or penetrating chest trauma. A hemothorax may also occur due to blood clotting defects, necrosis of the lung tissue, and as a complication of thoracic surgery; in these cases it occurs at first without a PTX also being present, but if left untreated hemothorax may result in a PTX[11, 17]. The diagnosis of a hemothorax may be made through a supine AP chest X-ray. It is usually seen as a diffused haze in the X-ray slide; 250 ml of blood is sufficient to cause a detectable blunting of the angle between the diaphragm and chest wall at the bottom of the thorax[11].

The treatment of a hemothorax consists of draining the accumulated blood from the pleural cavity. This is done by inserting a chest tube through the chest wall, usually between the 4^{th} and the 5^{th} rib, and applying suction[11]. After draining the pleural space, the visceral and parietal pleura are relocated back in their original position. The bleeding usually ceases after the pleural space is drained and the lung re–expands, but clotted blood must be removed[11]. A CT scan for a patient with a hemothorax is shown in Figure 1.2.

In a situation where microwaves are used for the detection of traumatic injury the presence of a hemorrhage is expected to have an effect on the net dielectric properties of anatomical structures[18]. A change in dielectric properties is the primary phenomena used to build a diagnosis through the use of diagnostic instrumentation which is based on microwaves. Therefore it becomes important to consider these injuries (pneumothorax and hemothorax) together in a situation where microwaves are used.

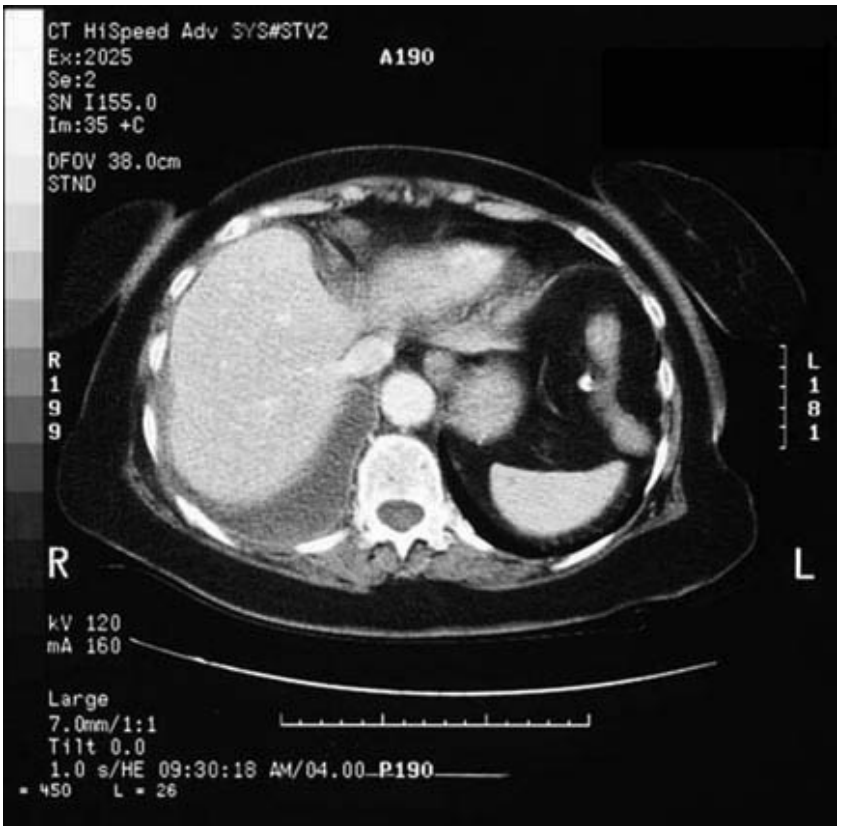

Figure 1.2: Contrast enhanced CT scan of a patient with right hemothorax(Source: M. C. Mancini, Hemothorax (Sep. 2012): `http://emedicine.medscape.com/article/2047916-overview`).

1.3 Microwaves in diagnostic medicine

The use of microwaves in diagnostic medicine has gained popularity in recent years due to developments in hardware and growth in computational power[19]. Devices that can detect cerebral hemorrhages through the use of broad spectrum microwaves are currently being developed[18, 20]. This system involves the incorporation of low frequency radio wave (or high frequency electromagnetic wave) antennas into a wearable helmet[20, 21]. The presence of a bleeding produces a measurable change in the readings made on a simplified human phantom[20]. Principals of detection that are employed in the microwave helmet (MWH), described in previous research projects[20, 21] have potential to be extended in order to detect the presence of air in the thorax. There is potential to develop a measurement modality that can exploit this property to diagnose PTX and hemothorax. Such a system would use a network of antennas similar to the one used in the MWH.

A handheld device which employs ultra wide band microwave pulses to detect a PTX, called PneumoScan, is in the final stages of clinical trials[9]. But developing a

wearable system which uses broad spectrum microwaves to diagnose chest trauma (using measurement instrumentation and detection principals similar to the high frequency electromagnetic wave technologies being currently used to detect traumatic brain injury) has an advantage over the PneumoScan that it has the potential for continuous monitoring of a patient. Microwave antennas can be incorporated into a belt or in any other wearable type sensor array. This antenna array can be connected to the same equipment that is used by the traumatic brain injury diagnosis system. In this way, there is potential to develop a versatile medical device that can be used to detect various types of traumatic injury, either at the scene of the accident or in the ambulance, while the patients are on their way to the hospital. These techniques may allow for better patient screening and reduce the time before which the patient receives treatment.

1.4 Microwaves and dielectric properties of materials

Microwaves are usually defined as electromagnetic waves in the frequency range 300 MHZ to 300 GHz, or with a wavelength, λ, between 1 m and 1 mm (in vaccum). Because of the high frequencies, standard circuit theory is not suitable to describe the propagation microwaves in material, instead Maxwell's equations must be consulted, Equations 1.1– 1.4[22].

$$\nabla \cdot \mathbf{D} = \rho \tag{1.1}$$

$$\nabla \cdot \mathbf{B} = 0 \tag{1.2}$$

$$\nabla \times \mathbf{E} = -\frac{\partial \mathbf{B}}{\partial t} - \mathbf{M} \tag{1.3}$$

$$\nabla \times \mathbf{H} = \mathbf{J} + \frac{\partial \mathbf{D}}{\partial t} \tag{1.4}$$

Where ρ is the electric charge density (C/m^3), $\mathbf{D}$ is the electric flux density (C/m^2), $\mathbf{B}$ is the magnetic flux density (Wb/m^2), $\mathbf{E}$ is the electric field (V/m), $\mathbf{M}$ is the magnetic current density (V/m^2) , $\mathbf{H}$ is the magnetic field (A/m) and $\mathbf{J}$ is the electric current density (A/m^2).

The following relations, Equations 1.5– 1.6, can be made between the electric current density, electric flux and electric field when the fields propagate through a material[22].

$$\mathbf{J} = \sigma \mathbf{E} \tag{1.5}$$

$$\mathbf{D} = \epsilon \mathbf{E} \tag{1.6}$$

Where σ is the total conductivity (S/m) and ϵ is the permittivity (F/m)[22]. The conductivity is a measure of the materials ability to conduct an electric current and the permittivity relates to the materials ability to transmit an electric field[22]. These are

referred to as the dielectric properties of materials. The permittivity of a material can be measured as relative permittivity, $\hat{\epsilon}$, expressed in Equation 1.7[23].

$$\hat{\epsilon} = \epsilon' - j\epsilon'' \tag{1.7}$$

Where, the real part ϵ', is the relative permittivity and the imaginary part, ϵ'', is the out of phase loss factor. The total conductivity can be calculated from Equation 1.8, with the knowledge of the imaginary part of the complex permittivity, ϵ''[23].

$$\epsilon'' = \sigma/\epsilon_0\omega \tag{1.8}$$

Where σ is the total conductivity of the material, $\epsilon_0 = 8.854\times10^{-12}\ F/m$ is the permittivity of free space and ω is the angular frequency of the field.

1.5 Microwave measurements

Microwaves are electromagnetic radiation and transmission of this electromagnetic radiation through an electrical network is governed by scattering parameters or s-parameters of the network under consideration[22]. The s-parameters, in very simplified terms, are the net effect the dielectric properties of a transmission system (mentioned in the previous section) have on a voltage incident on the system. They are represented as elements of a the scattering matrix presented in Equation 1.9.

$$\begin{pmatrix} V_1^- \\ V_2^- \\ \vdots \\ V_N^- \end{pmatrix} = \begin{pmatrix} S_{1,1} & S_{1,2} & \cdots & S_{1,N} \\ S_{2,1} & S_{2,2} & \cdots & S_{2,N} \\ \vdots & \vdots & \ddots & \vdots \\ S_{N,1} & S_{N,2} & \cdots & S_{N,N} \end{pmatrix} \begin{pmatrix} V_1^+ \\ V_2^+ \\ \vdots \\ V_N^+ \end{pmatrix} \tag{1.9}$$

The scattering matrix is a description of network, with N ports (input/output points), from the point of view of its ports and relates the voltages incident, V_1^+, and reflected, V_1^-, on the ports. A particular element of the scattering matrix, $S_{ij} = S_{ji}$, can be found by Equation 1.10.

$$S_{ij} = \left.\frac{V_i^-}{V_j^+}\right|_{V_k^+=0 for K\neq j} \tag{1.10}$$

Where S_{ij} is the transmission signal between port i and port j, and S_{ii} is the reflection coefficient looking into port[24]. This type of representation is useful when working with a network that operates at higher frequencies, as it is harder to measure total voltages and currents at higher frequencies but easier to measure incident and reflected voltages[24]. Scattering parameters can be measured using device called a vector network analyser. Changes in the anatomical structures of the human body can result in changes in its dielectric properties; These changes will in turn result in changes in the s-parameters, which can be measured using a network analyser device. Therefore a change in the

human body's anatomy, like the presence or absence of air in the pleural cavity in the case of a PTX will ultimately result in a measurable change in the resulting s-parameters, measured in the two scenarios. It is this change that can be used to detect a condition like a PTX using microwaves.

1.6 Aim

The aim of this master's thesis is to investigate the potential of microwaves based technologies, specifically technologies that use s-parameter analysis,to detect a traumatic PTX. This investigation will include the construction a realistic phantom of the human thorax, and in it modelling the most common traumatic thorax injuries–PTX and hemothorax. The goal also involves the construction of a wearable microwave instrument to perform measurements on the thoracic phantom. The collected measurement data will then be analysed, using an in-house classifier, for the verification of effectiveness of the developed measurement system.

The aim can be summarised as:

- Construct a realistic phantom of the human thorax; in terms of size, anatomy, and dielectric properties.
- Model pneumothoraces of different sizes in the thoracic phantom.
- Model a hemothorax in the developed phantom.
- Construct a wearable measurement device.
- Evaluate the detection accuracy for PTX of different sizes, and when a hemothorax is present, using the available classifier.

The work will be done under the following constraints, and assumptions:

- The phantom needs to be developed under constraints of time, and cost. Therefore, the phantom would provide an approximation of the human thorax; in that it will only represent the most prominent thoracic features, which are relevant to the analysis done in this study.
- The study will use instrumentation and measurement devices, and software tools that have been previously developed for applications similar to, but not the same as, this analysis. The available tools included a dielectric probe kit, a PNA, microwave antennas, and all the software needed to interface and control this hardware.
- The analysis of the measurement data will be done using an in-house classifier which had been previously developed by a different research group. No other data classification methodology will be used to separate the data from different measurement sets.
- For the purpose of statistical analysis, and the median filtering of data, existing functions available in the computational tool MATLAB will be used.

2

Materials and Methods

This section describes the process through which the measurement principle was developed and verified. A realistic phantom of the human thorax was constructed using liquids with appropriate dielectric properties placed in containers that accurately represented, with acceptable approximations, the geometry of the human chest cavity. This section starts by explaining the physical properties of the biological tissue which the phantom needed to replicate and describes the procedures, and the instrumentation that were used to quantify the dielectric properties of various materials. Furthermore, it describes how a wearable antenna array was developed.

2.1 Measurement of dielectric properties

In order to measure the dielectric properties of the liquid solutions used for the thorax phantom, the Agilent[1] programmable vector network analyzer (PNA) was used together with the Agilent dielectric measurement probe kit, 85070E at the Microwave lab of the Signals and System Department, Chalmers. The solutions were measured to verify that they correctly represented the dielectric properties of the various tissues located inside the thorax cavity.

The PNA had to be turned at least 30 minutes prior to each lab session, as it needed to be warmed up in order to get reliable measurement results. The dielectric measurement probe was mounted on a stand in a very stable fashion and was not moved during any measurement to ensure that the measured results were not affected by any movement artifacts. The probe was connected with one of

[1] Agilent Technologies, Santa Clara, CA, United States

the PNA in-ports through a cable, and it was calibrated before each session. The complete setup can be seen in Figure 2.1. The calibration was performed using existing software on the PNA. The software asked for calibration type, the temperature of deionised water (which was needed for the calibration), the frequency range, and the number of measurement points. The calibration software asks the user to perform three tests; open probe, (i.e. measure in air), short circuit the probe with a small piece of aluminium foil, and measure deionised water (of the temperature). The test results were verified by a polar plot generated by the software. The relative permittivity, and the total conductivity can then be calculated with the imaginary part of the measured permittivity, using equations 1.7 and 1.8.

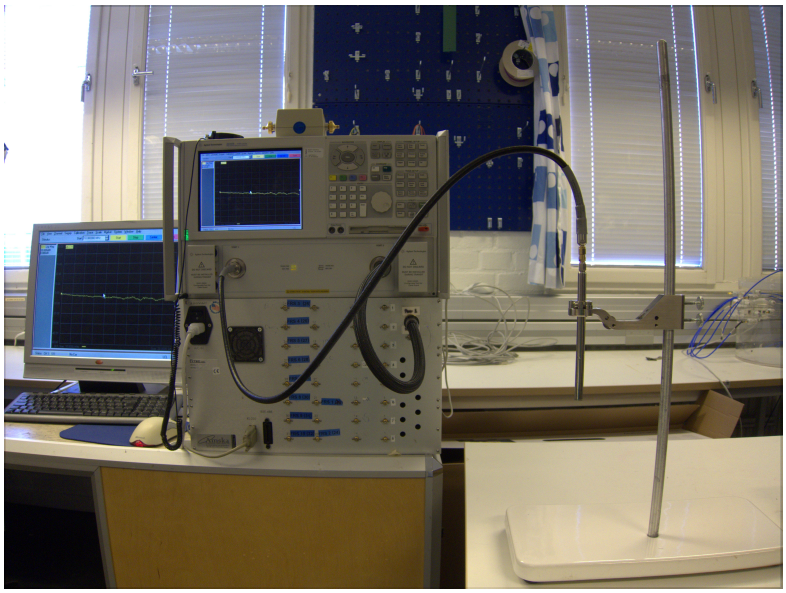

Figure 2.1: The setup for measurements of dielectric properties, with the PNA to the left and the dielectric probe to the right.

2.2 Microwave measurements

In order to make microwave measurements, the PNA was used together with a switching box (CXM/ 128-5-W), to handle multiple inputs to the PNA. The PNA was connected to the switch through two ports using special coaxial cables, extension cables to the antennas could then be attached to the outputs of the switch box. All microwave measurements were conducted at the Microwave lab, Signals and system department, Chalmers. All microwave measurements were done in the frequency range 100 MHz to 3 GHz, at 401 frequency steps with a step-size of 7.25 MHz. The format of the output data was scattering parameters as listed in Equation 1.10, presented as complex numbers.

The PNA was calibrated using an Agilent Electronic Calibration module (ECal) together with an in-house MATLAB program that facilitates the calibration process. The MATLAB program allows the user to select measurement parameters and guides the user through the calibration process, i.e. tells the user which cables to connect to the ECal module.

2.3 Phantom construction

In order to construct a human thorax phantom that can model common thorax injuries, various sources of information have been consulted to arrive at the requirements for the simplified model. Sources have been consulted [23, 25, 26] to obtain the dielectric properties of the various biological tissues found in the human thorax, at 1 GHz, listed in Table 2.1. Phantom solutions consisting of a mix of deionised water and ethanol were created and their permittivity and conductivity was matched to the dielectric properties of biological tissue at 1 GHz. The goal was match the relative permittivity as closely as possible to biological tissues and to keep the total conductivity values as close as possible to those of biological tissues, presented in the existing literature.

Table 2.1: Dielectric Properties of Biological Tissues [23, 25, 26]

Organ	Relative Permittivity (F/m) (at 1 GHz)	Conductivity (S/m) (at 1 GHz)
Skin	40.9	0.9
Fat	5.5	0.05
Muscle	54.8	0.98
Bone	12.3	0.16
Cartilage	42.3	0.84
Inflated Lung	21.8	0.44
Blood	61.1	1.58

In order to represent the dielectric properties of the biological tissues in the human thorax, so that pneumothoraces and hemothoraces of different sizes could be modelled, three different solutions were created. The first solution represents the dielectric properties of the thorax excluding the lungs. The solution was created by calculating the mean permittivity of skin, fat, muscle, bone and cartilage tissue from Table 2.1. Organ volume was not taken into consideration, due to size

variations between individuals. This solution is referred to as the thorax solution or solution 1. The second solution represents the dielectric properties of a inflated lung from Table 2.1. The dielectric properties of the inflated lung varies for different degrees of inflation [23]. This solution is referred to as the lung solution or solution 2. The third solution represents the dielectric properties of blood, from Table 2.1, and is referred to as the blood solution or solution 3.

To arrive at solutions of the necessary permittivity various mixtures of ethanol and deionised water were tested. Beginning with a 1:1 mixture of water (permittivity of 80 at 20 $°C$) and ethanol (24.3 at 25 $°C$) a solution was created and its relative permittivity measured. Then the relative permittivity of this solution was subsequently raised or lowered, as desired, by adding a measured amount of water or ethanol. This process was repeated until a solution of desired relative permittivity and conductivity was obtained. The final compositions of the created solutions have been listed in Table 2.2.

Table 2.2: Final composition of the created phantom solutions [23, 25, 26]

Solution Name	Composition (water:ethanol)	Relative Permittivity (F/m) (at 1 GHz)	Conductivity (S/m) (at 1 GHz)
Thorax solution	1:5	30.5	0.55
Inflated lung solution	1:20	21.6	0.44
Blood solution	1:0.58	60.8	0.38

The outer borders of the human thorax phantom was represented by a large container that was approximately shaped as a human thorax, B1 in Figure 2.2. The lungs were represented by thin plastic cylinders, C1 and C2 in Figure 2.2, placed side by side inside the large bucket, and taped down to the bucket so that hey would not move, see Figure 2.3 (a). The volume of the plastic cylinders was 2 liters which is an upper approximation of the lung volume of a typical healthy 25 year old (Swedish) male of of height 177 cm. This value is an approximation made using the value of vital capacity[1], residual volume, and thoracic independent volume of an adult male [27]. Equations 2.1– 2.2 show the variation of vital capacity (VC) with age and height for a healthy human, male and female [27].

$$VC_{male} = (27.63 - 0.112 \times age) \times height \tag{2.1}$$

[1]Vital Capacity is the maximum amount of air a person can expel from the lungs after a maximum inhalation

$$VC_{female} = (21.78 - 0.101 \times age) \times height \tag{2.2}$$

The total lung capacity is defined as the sum of VC and the residual volume[2] (15 ml/kg). Thus the total amount of air that is present in the lungs is the sum of the VC and the residual volume. This volume is called the total lung capacity. Now the thoracic independent volume is defined as the volume of the thorax cavity when it is at a state where the thoracic cavity's elastic forces are at equilibrium with the lungs inward elastic forces. This value is defined to be 70% of total lung capacity. For a male of the given height, weight, and age this works out to be about 3.811 litres (this is the total value for both the lungs). Thus each lung was taken to be 2 litres each as the commercially available cylinders of the most suitable dimensions had a volume of 2 liters.

The large container was almost fully filled with the thorax solution and the content of the cylinders depended on the injury that was modelled. This setup with two cylinders allows for different thorax injuries to be modelled by simply changing the content of the cylinders. For a healthy phantom both cylinders were completely filled with the inflated lung solution. For a PTX one of the cylinders, depending on which side the PTX was located, was filled with the inflated lung solution. The other cylinder was empty with a balloon hanging from the top. The balloon was filled with the inflated lung with a volume that corresponded directly to the size of the PTX. The PTX size is the volume of air left after the balloon is introduced in the cylinder, i.e. to model a PTX of size 25%; the balloon was filled with 1.5 litre of the inflated lung solution. In order to model a hemothorax, the same setup was used as for a PTX but with blood solution added into the cylinder with the hanging balloon (filled with the needed quantity of the inflated lung solution). The filled cylinders were sealed with tape so no liquid would leak out during measurements. The large bucket and cylinders, healthy and 20% PTX, can be seen in Figure 2.3.

2.4 Microwave antennas

Microwave antennas were used to transmit and receive the signal generated by the PNA across the test medium (a thoracic phantom or an actual human thorax). Figure 2.4 shows the geometry of the antennas that were used.

These patch antennas were used because they are economical in terms of their size, weight, and cost. They are thus named because the antenna consists of a triangular metallic patch placed on top of a dielectric substrate, which is in turn attached onto a ground plate. The antenna has been shown to work well in a frequency range

[2]Residual Volume is the amount of air left in the respiratory organs after a maximum possible exhalation.

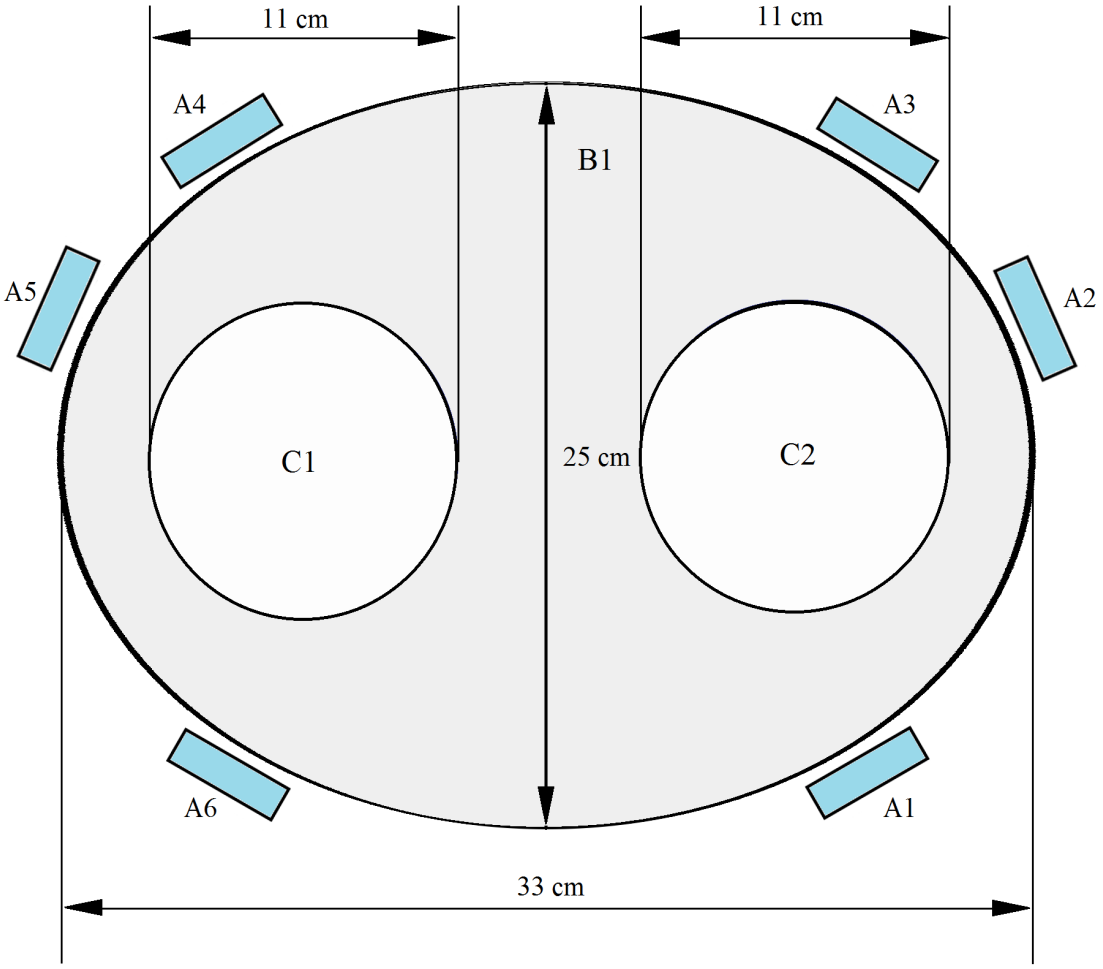

Figure 2.2: Schematic of the human thorax phantom (B1 is thorax cavity, C1 and C2 are the lung spaces) and approximate position of the microwave antennas(A1–A6).

of 100 MHz to 3 GHz; through the use of a suitable coupling material between the antenna patch and the test medium, and by introducing a v–shaped slot in the patch. These antennas have been previously used, with good results, in other research work; employing a similar use of microwaves for measuring injury induced changes in dielectric properties of regions in the human body [18, 20, 21]. They were therefore found to be suitable to make the measurements needed for this thesis work.

Figure 2.3: Pictures of: (a) A cylinder modelling a healthy lung (b) A cylinder modelling a 20% PTX (c) Assembled thorax phantom (d) Setup for continuous measurements of a decreasing PTX.

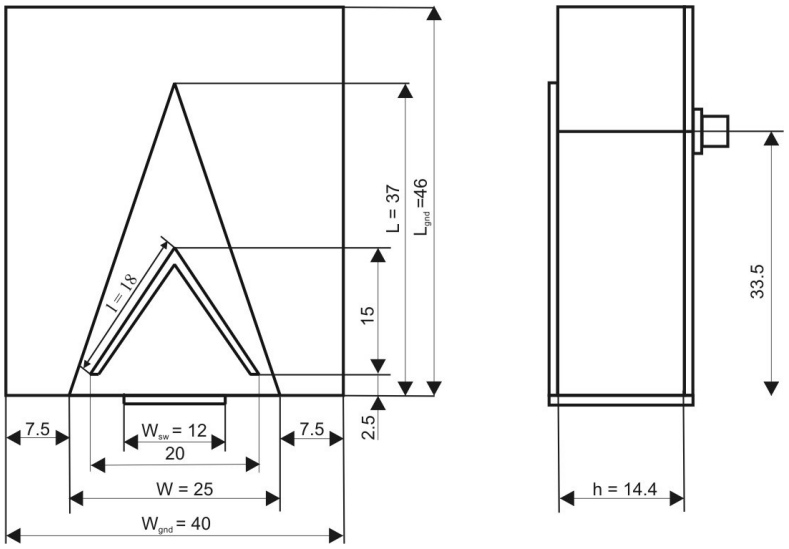

Figure 2.4: Geometry of the microwave antenna (Source: Antennas and Propagation Society International Symposium, 2008. AP-S 2008. IEEE).

2.5 Antenna belt

The antennas needed to be held in place on the test subject while measurements were being made. The placement of the antennas during measurements also needed to be consistent. For these reasons the antennas were incorporated into a belt. The belt was a rectangular strip of synthetic leather to which the antenna were tied using plastic tie rods. The belt also served the purpose of providing physical protection to the antennas. Figure 2.5 illustrates the antenna arrangement around the human thorax. Two antennas were placed on the front, two on the sides, and two antennas were at the back of the test subject (not seen in Figure 2.5), diametrically opposite to the antennas in the front.

The belt was developed in two iterations. The first version of the belt contained 4 antennas placed at the level of the seventh rib on the front and lateral part of the thorax, on both the left and right side. These positions were chosen as a survey of available literature showed that in the the case of a supine trauma patient most pneumothoraces start to progress from the lower front part of the chest [10, 28]. In this location there is a minimum of muscle and adipose tissue between the antennas and the lungs. Self adhering pads of Silipos gel were placed on the antennas. These served the dual purpose of providing a soft interface between the antennas and the subject being measured, while also providing some mechanical protection to the antennas. Preliminary measurements were made with this four–antenna belt to verify the validity of the transmission signals obtained through measurements on the phantom. This was done through a visual inspection

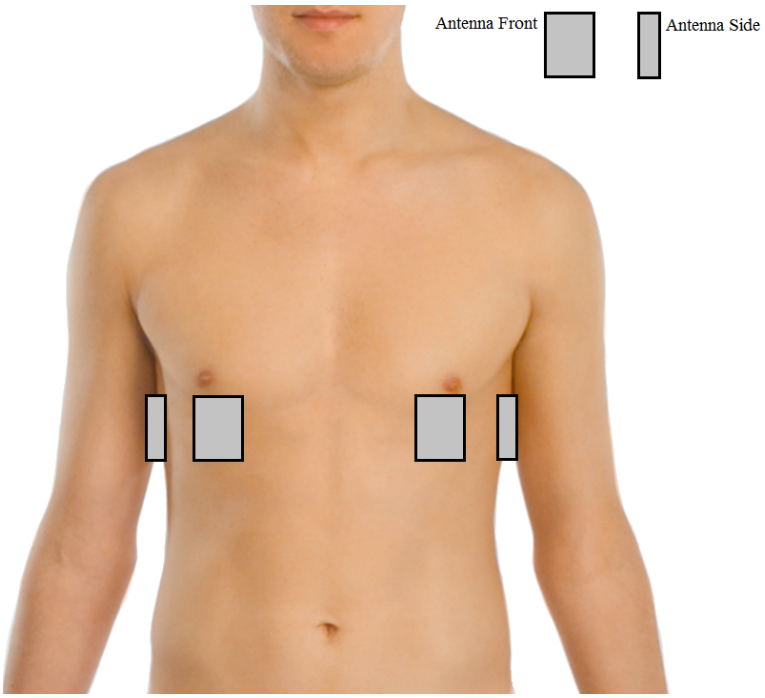

Figure 2.5: Schematic of antenna placement (modified from wikimedia commons [29]).

of the data obtained through measurements on the phantom and the data obtained through measurements made on a human test subject. In the second version of the belt two antennas were added in addition to the four antennas present in the first version of the belt. The two extra antennas were added so that they would be on the back of the subject being measured, just under the scapula, on the level of the seventh rib. These antennas were added to collect useful information about how the anterio-posterior transmission signal changed in the presence of a PTX. The belt was also provided with extra holes at the back so that it could be fastened securely test subjects whose circumferences differed.

2.6 Verification of phantom characteristics

Upon measurement, the PNA generated a measurement matrix M with complex values representing the s-parameter data, of the form $M(m,n,f)$. Where m and n were the indices of the sending and receiving antennas, respectively. For a 4 antenna belt they varied from 1 to 4, and for a six antenna belt they varied from 1 to 6. The matrix index f denoted the frequency point for which the measurements were made; f varied from 1 (100 MHz) to 401 (3 GHz), with each increment in index representing a step in frequency of 7.232 MHz. To verify the validity of the thoracic phantom, measurements made on the phantom were compared with mea-

surements made on a human test subject. This comparison was done by plotting the magnitudes of the s-parameter data over all 401 frequency points, for a fixed sending and receiving antenna pair. The plots thus generated were compared for a similarity in the shape of the envelop, and the order of magnitude of the absolute values over different frequency points. The goal was to asses the similarities and the dissimilarities between data collected from the phantom representing a healthy human, and data collected from a healthy human test subject; so as to ascertain to what extent the phantom could mimic the human thorax, as a transmission channel. To improve the clarity of the plots, data was median filtered (for a fixed antenna pair $[M,N]$, over the entire frequency range), with frequency points (f) in the interval ω, around a centre frequency point (f_c) using the Equation 2.3.

$$y[M,N,f_c] = median(x[M,N,f]), f\epsilon\omega \tag{2.3}$$

Where M,N were a set of fixed indices, f varied from 1 to 401, and ω was the number of points in the neighbourhood of the data point in questions, which were considered for median filtering.

2.7 Microwave measurements on thorax phantom

Measurements were conducted on PTX of different sizes on left and right lung, hemothorax on left and right lung and on healthy lungs. The total amount of measurements for each setup is listed in Table 2.3. It was not feasible to conduct all measurements at one session due to time restrictions and limited amount of cylinders (the lungs had to be fabricated before the measurement session, for practical reasons) instead the measurements were conducted over two sessions.

Table 2.3: Thorax phantom measurements

Setup	Number of measurements
Left PTX 10%	30
Right PTX 10%	30
Left PTX 20%	30
Right PTX 20%	30
Left PTX 50%	30
Right PTX 50%	30
Left 250 ml hemothorax	30
Right 250 ml hemothorax	30
Healthy lungs	60

To most accurately compare the data measured on the different setups the impact from time-dependent possible sources of bias (such as temperature induced drifts) was minimised by randomising the measurement order by using a MATLAB random generator script. Three consecutive measurements, referred to as a triplicate, were made on each setup in order to have redundancy in the measurements, before the next was randomly selected, this was repeated until all measurements had been collected for all of the setups. In between triplicates the antenna belt was removed and reapplied at a new position; also randomly selected using a MATLAB random generator script. The bucket was marked with a reference point, the belt was placed; above, over, at the reference point, rotated 10° to the left or rotated 10° to the right from the reference point. This was done to incorporate variability due to that the belt position will vary some from patient to patient. In this way the test measurement was completely randomised, to the extent possible. However due to time constraints, and the fact that there was a limited number of cylinders all measurements could not be made over the same measurement session, i.e., on the same day. To take into account any variation that not making the measurements on the same day may have on the collected data, the measurement instrument ion (the PNA) was re-calibrated before each measurement session. Some test measurements were also made before the start of each measurement session, to ensure that there were no damaged cables and that the measurement system was functioning correctly.

2.8 Measurement on progressively decreasing pneumothorax

Measurements were made on a decreasing PTX, connecting a pump to a balloon inside the cylinder. The setup can be seen in Figure 2.3 (d). First off, 30 measurements were made with the entire cylinder filled with air (100% PTX in the lung). The balloon was then filled (using the pump connected to the balloon), in steps of in 300 ml with the inflated lung solution; this was done till the balloon was filled with 1200 ml of solution, see Table 2.2. At each volume step, nine measurements were made. Lastly, the balloon was filled upto 1500 ml, and a set of 30 final measurements were made. Table 2.4 includes all measurements that were made on the decreasing PTX. The first 30 and the last 30 set of measurements, i.e., the measurements made a balloon the container when the balloon was completely empty (100% PTX), and with the balloon filled to 1500 ml in size (25% PTX) were used as baseline measurements during analysis of this measurement series–simulating a 100% PTX, decreasing to a 20% PTX.

Table 2.4: Continuous measurement of a decreasing PTX from 100% to 25%

PTX size	Balloon volume	Number of measurements
100%	0 ml	30
85%	300 ml	9
70%	600 ml	9
55%	900 ml	9
40%	1200 ml	9
25%	1500 ml	30

2.9 Classification

A classifier based on singular value decomposition was used to analyse the data gathered [18]. The classification begins with a re-arrangement of the measurement data, from a three dimensional matrix into a one dimensional vector. The classifier then, first, breaks down the measurement data, into linearly independent components using singular value (SVD) decomposition of the re-arrangement measurement data. A singular value decomposition of a matrix M of dimensions (m,n), denoted by M_{mn}, is a factorisation of the form shown in Equation 2.4.

$$M_{mn} = U_{mm} S_{mn} V_{nn}^{T} \tag{2.4}$$

Where U_{mm} and V_{nn} are the orthonormal matrices containing eigenvectors corresponding to the eigenvalues for MM^T and M^TM, respectively. $S = \begin{pmatrix} D & 0 \\ 0 & 0 \end{pmatrix}$, where D is a diagonal $r \times r$ matrix, with $r = rank(A)$. D has the square roots of the positive eigenvalues from either U_{mm} or V_{nn}, in descending order. The values in S represent the decomposition of the matrix M_{mn} into subspaces of orthonormal basis vectors. This decomposition can be used to asses how similar measurements are, either to each other, or to a subspaces made using the SVD of several measurement points. For classification, the leave one out approach was used. Wherein, each measurement point was analysed in turn by comparing it to subspaces made using SVD decomposition, from measurements collected made on different kinds of phantoms.

3

Results

This chapter lists the results of the development of the belt, and its validation on the thoracic phantom.

3.1 The microwave antenna array belt

The microwave antenna array belt is shown in Figure 3.1, which shows the antennas, covered with Silipos gel pads, attached to the leather backing which forms the strap of the belt.

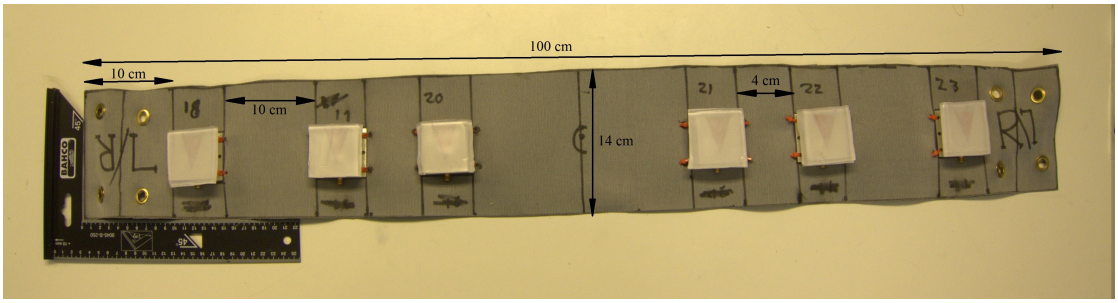

Figure 3.1: The microwave antenna array belt showing the, with some important dimensions noted.

The belt dimensions were symmetrical, i.e., the various distances on the left side were the same as the distances on the right side. The two sets of holes provided in the belt allowed it to be tightly fasted around subjects of differing girths. The belt can be seen fastened around a human test subject in Figure 3.2.

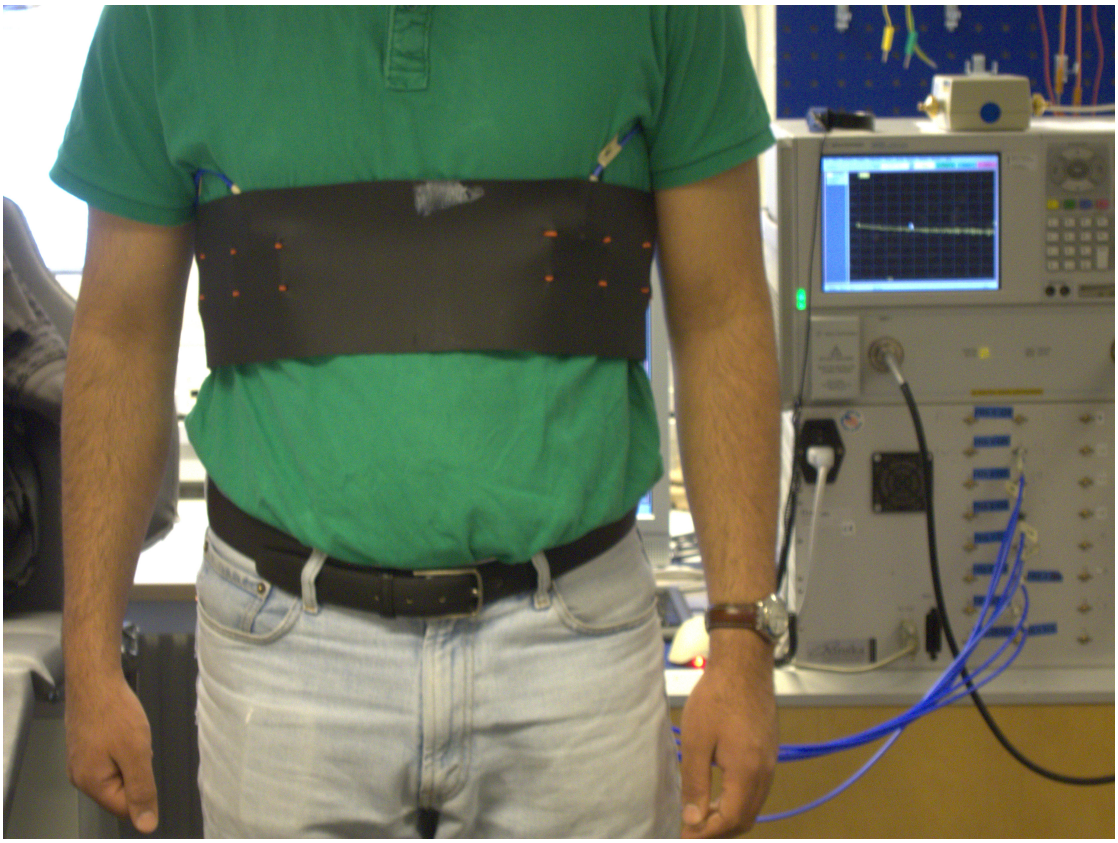

Figure 3.2: The microwave antenna array belt fasted around a human test subject.

3.2 Attenuation in the thorax phantom.

The absolute value of measurements from a healthy thorax phantom and a healthy human subject were calculated and median filtered, with window size 15. The mean of the median filtered measurements was then plotted against each other in Figures 3.3(a) and 3.3(b) .

3.3 Reproducibility test of the phantom solutions

To verify the reproducibility of the phantom solutions, all the three solutions were reproduced three times and the dielectric properties for each solution was measured three times with the dielectric probe. The solutions were produced and measured in a random order.

The standard deviation of the permittivity and conductivity was calculated in MATLAB, and compared to published results from Table 2.1, for each solution in

order to verify the realism and reproducibility of the phantom solutions. The results for the three solutions are presented in Figures 3.4(a)- 3.4(f).

3.4 Data analysis

3.4.1 Fixed pneumothoraces

The SVD based classification algorithm was used to analyse the data collected from measurements made on the thoracic phantom. Measurements were made over three measurement sessions, on three different days. Table 3.1 lists the measurement number corresponding to different phantoms, the attributes of the phantoms, and the day the measurements were made on.

Table 3.1: Details of measurements made on phantoms with pneumothoraces of fixed sized

Measurements	PTX Size (Side)	Measured on
1–30	10% (Left)	Day 2
31–60	10% (Right)	Day 1
61–90	20% (Left)	Day 2
91–120	20% (Right)	Day 2
121–150	50% (Left)	Day 1
151–180	50% (Right)	Day 2

Each of the 180 measurements listed in Table 3.1 were compared to two subspaces, constructed using singular value decomposition. The first subspace was made from the 60 measurements made on phantoms mimicking a healthy patient. The second subspace was made using the measurements on the phantoms with a PTX with the triplicate set of the measurement point being analysed, left out. Thus the second subspace was made from 177 measurements. Figure 3.5 shows the result of this analysis.

3.4.2 Hemothorax

The final set of results presented are from the analysis of measurements made on phantoms with a 50% PTX and a hemothorax, present in the same lung (designated, hemothorax phantom). Data from the hemothorax phantom was compared to phantoms with a 50% PTX, and phantoms mimicking a healthy patient; using the SVD classifier. The results of this analysis are given in Figure 3.6 and Figure 3.7.

Figure 3.6 shows the distances of measurement points representing data from a phantom with a 50% PTX, from SVD subspaces constructed using data from the hemothorax phantoms, and data gathered on a phantom with no PTX. In Figure 3.7 the distance of the measurement points from the hemothorax phantoms are calculated from SVD subspaces made from the hemothorax phantoms, phantoms with a 50% PTX, and phantoms representing a healthy patient.

3.4.3 Progressively decreasing pneumothorax

The next set of measurements were made on a phantom with a progressively decreasing PTX, in the absence of all possible variations between measurement sets. Details of the measurements analysed are listed in Table 3.2. Starting with a large PTX (100%) present on one side (in this case the right side), taken as the upper baseline. The size of this PTX was progressively decreased in fixed steps and measurements for each step were made for each step until a final, minimal PTX size was reached (25%), this was taken as the lower baseline.

Table 3.2: Details of measurements made on phantoms with a progressively decreasing PTX

Measurements	PTX size
1–9	100%
10–18	85%
19–27	70%
28–36	55%
37–45	40%
46–54	25%

This data was compared to two baseline subspaces–the first was 20 measurements made on a phantom with a large, 100% PTX, and the second was 20 measurements made on a phantom with a small, 25% PTX. The results of this analysis are shown in Figure 3.8. All measurements, i.e., the two baselines, and the decreasing PTX measurements, were made on the same day.

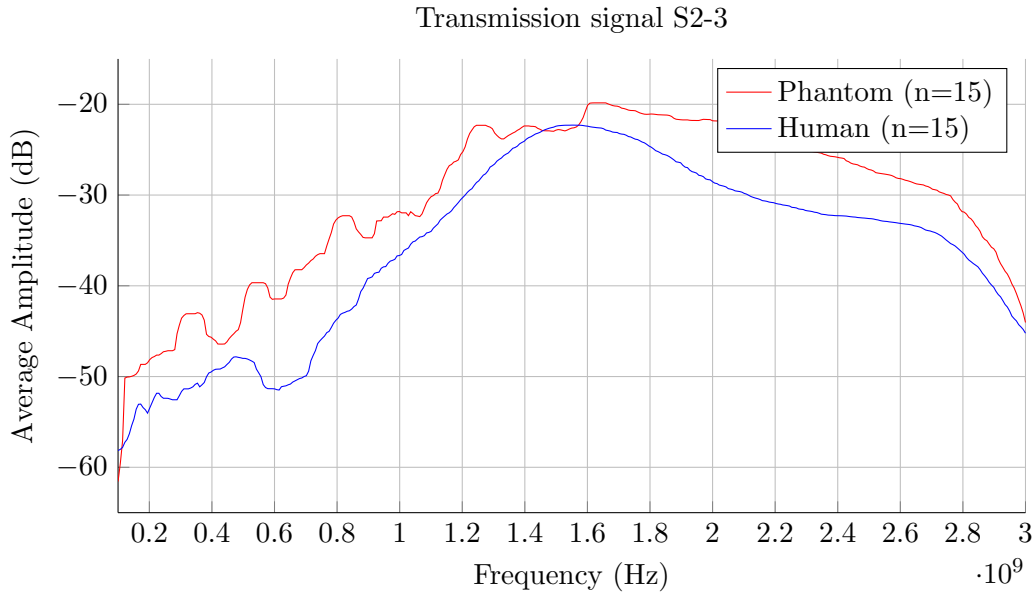

(a)

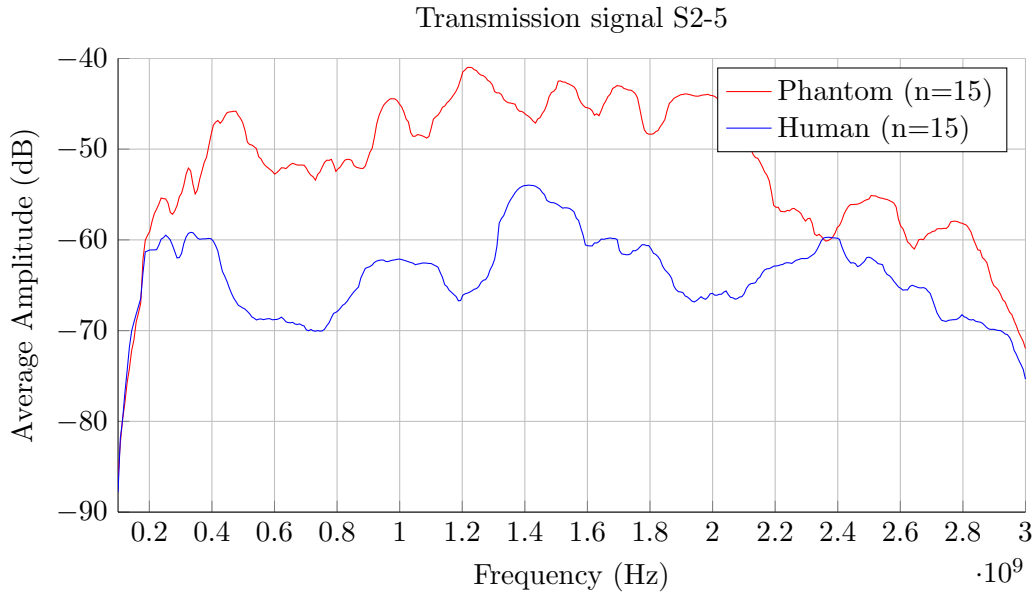

(b)

Figure 3.3: (a) Transmission signal across two closely located antennas (b) Transmission signal across the thorax. The phantom configuration was chosen to simulate a healthy person. These results were representative for similar transmission signals and for different human subjects.

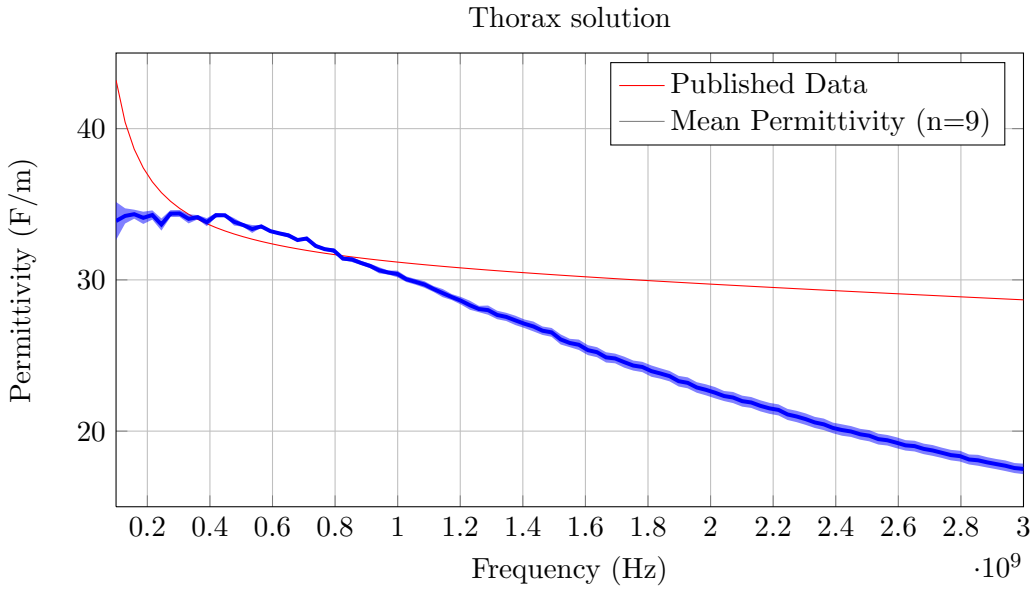
Thorax solution
Published Data
Mean Permittivity (n=9)
Permittivity (F/m)
40
30
20
0.2 0.4 0.6 0.8 1 1.2 1.4 1.6 1.8 2 2.2 2.4 2.6 2.8 3
Frequency (Hz)
·10^9

(a)

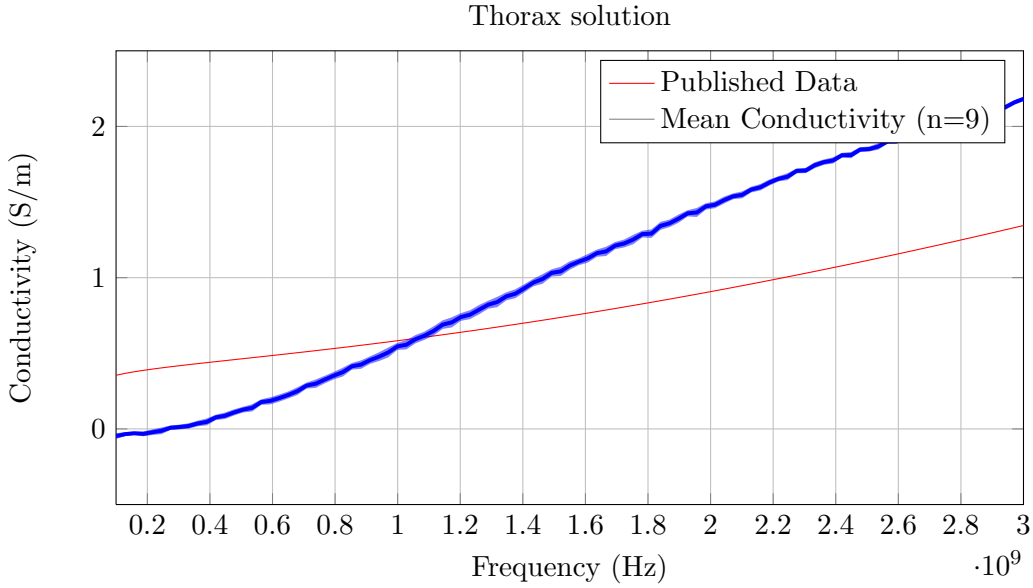
Thorax solution
Published Data
Mean Conductivity (n=9)
Conductivity (S/m)
2
1
0
0.2 0.4 0.6 0.8 1 1.2 1.4 1.6 1.8 2 2.2 2.4 2.6 2.8 3
Frequency (Hz)
·10^9

(b)

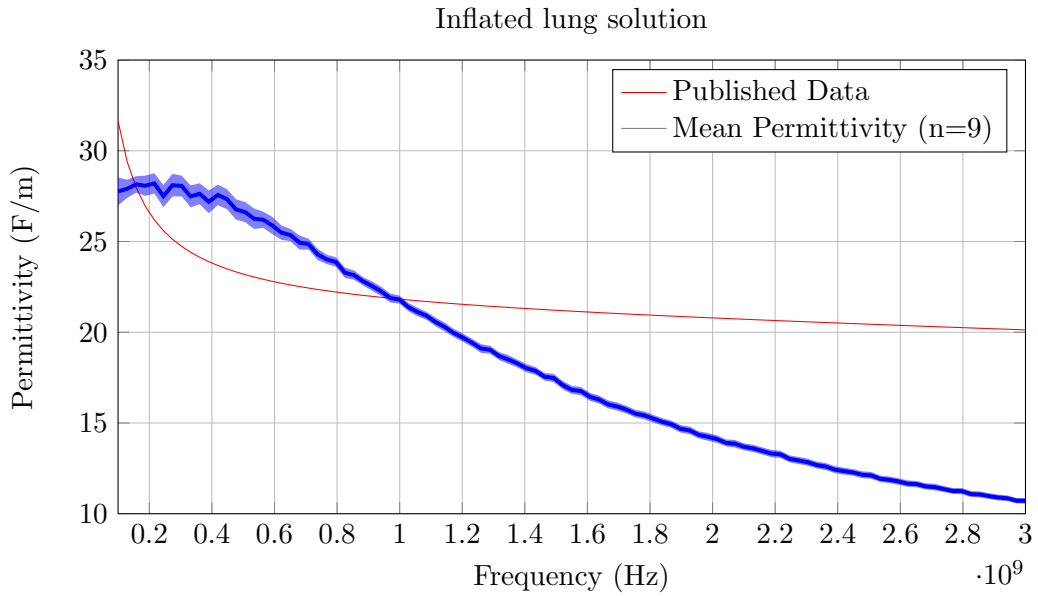
Inflated lung solution
Published Data
Mean Permittivity (n=9)
Permittivity (F/m)
35
30
25
20
15
10
0.2 0.4 0.6 0.8 1 1.2 1.4 1.6 1.8 2 2.2 2.4 2.6 2.8 3
Frequency (Hz)
·10^9

(c)

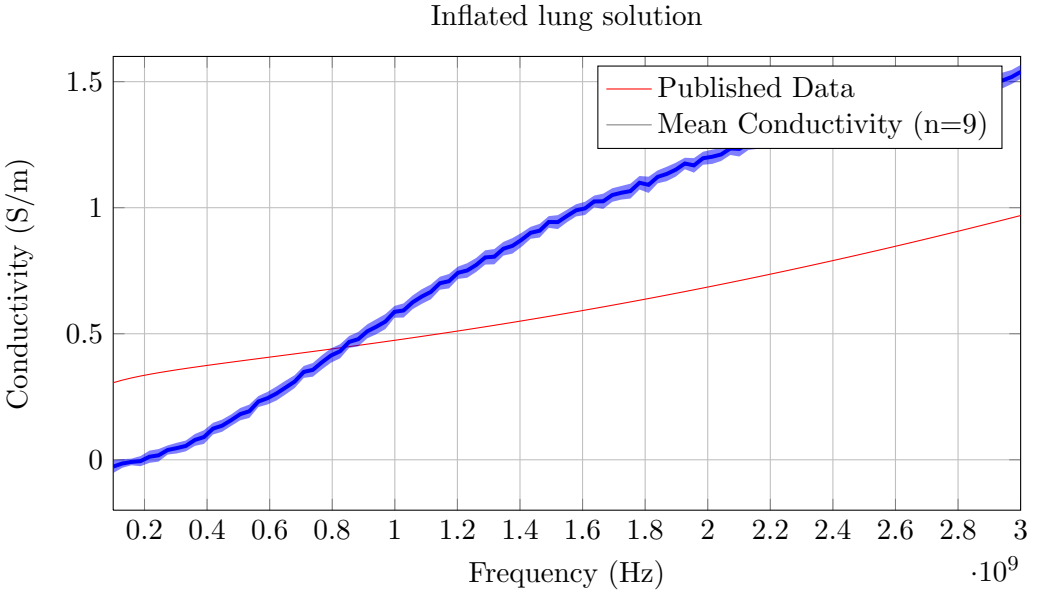
Inflated lung solution
Published Data
Mean Conductivity (n=9)
Conductivity (S/m)
1.5
1
0.5
0
0.2 0.4 0.6 0.8 1 1.2 1.4 1.6 1.8 2 2.2 2.4 2.6 2.8 3
Frequency (Hz)
·10^9

(d)

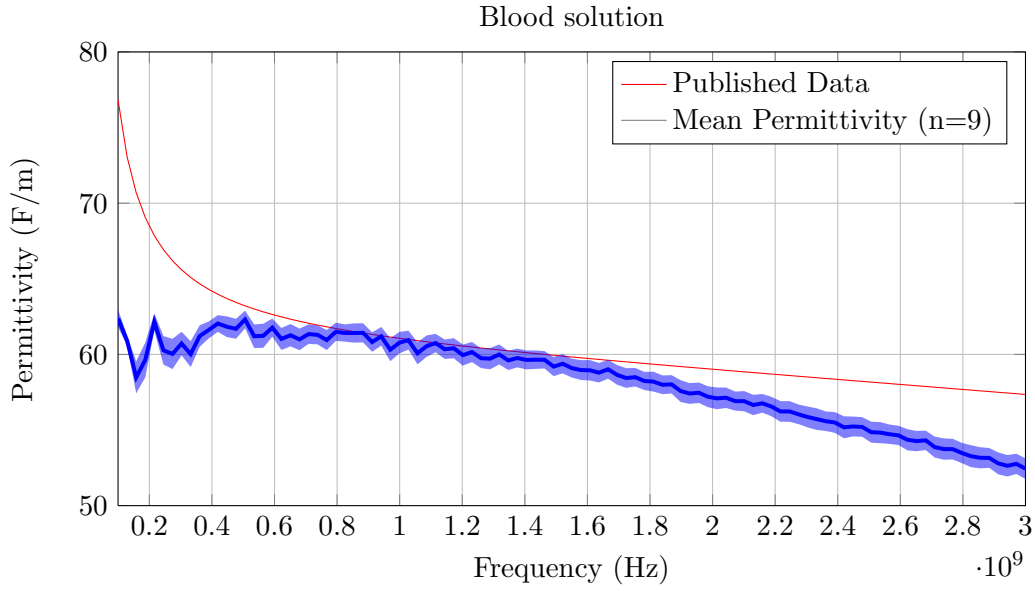

(e)

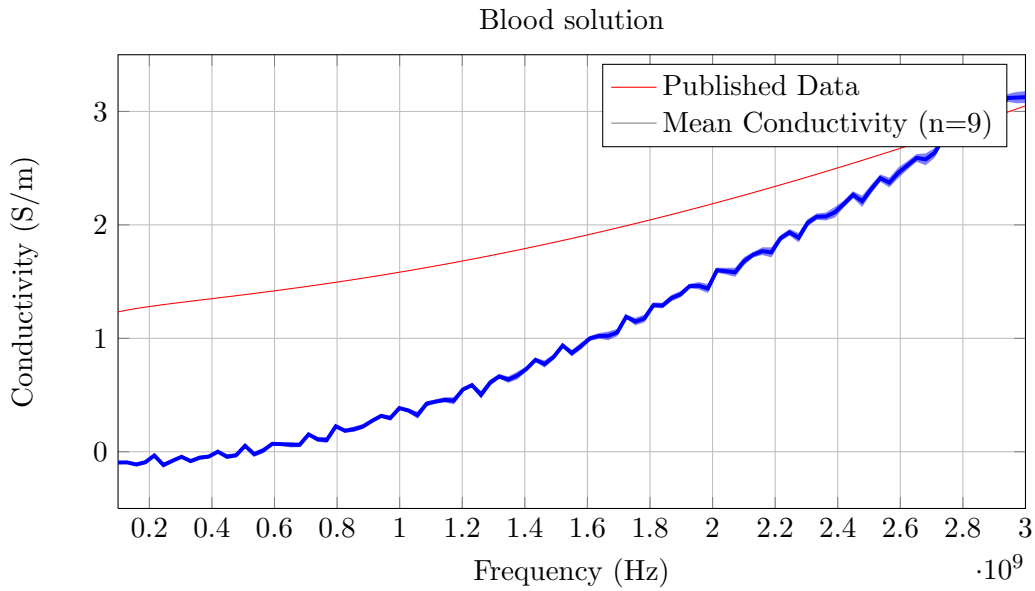

(f)

Figure 3.4: (a) The permittivity of the thorax solution (b) The conductivity of the thorax solution solution (c) The permittivity of the inflated lung solution (d) The conductivity of the inflated lung solution (e) The permittivity of the blood solution (f) The conductivity of the blood solution solution.

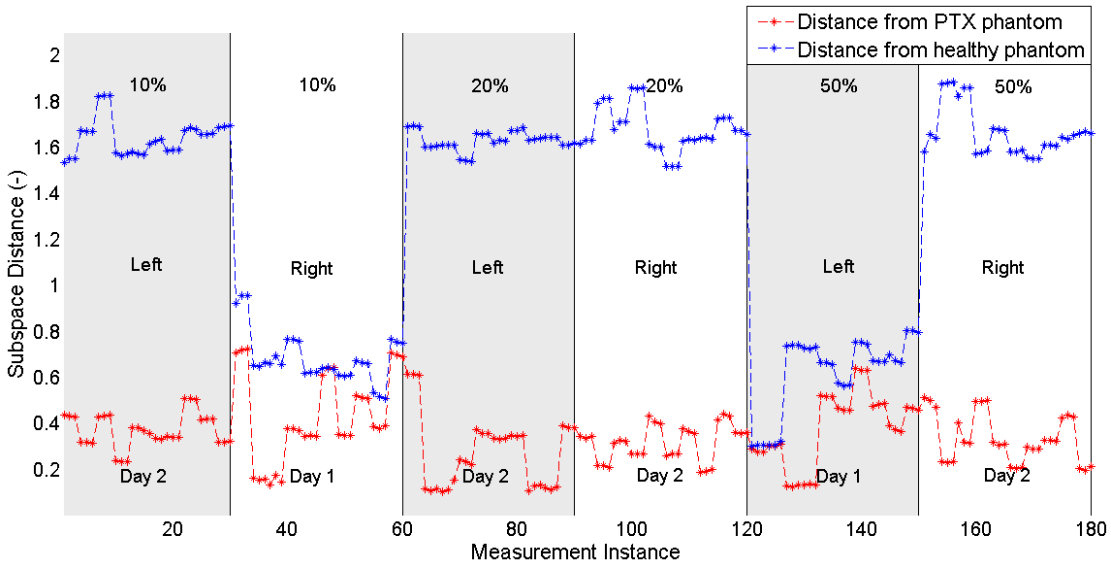

Figure 3.5: Results of analysis of measurements made on pneumothoraces of fixed sizes, measurement days, and PTX size and location have also been illustrated.

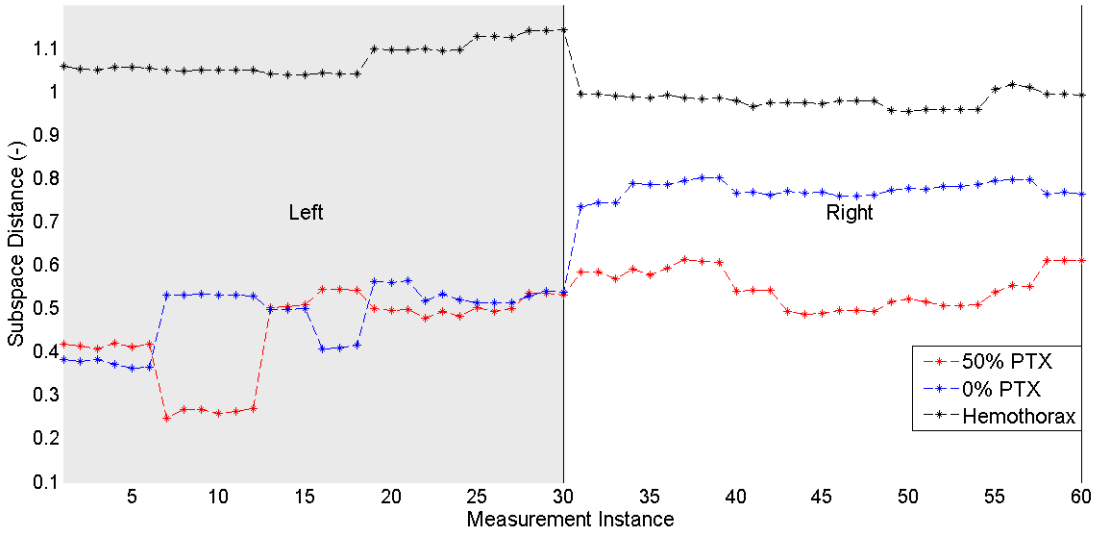

Figure 3.6: SVD subspaces distance of hemothorax phantom measurements, to subspaces of data gathered from 50% PTX phantoms, phantoms mimicking a healthy, and the hemothorax phantoms.

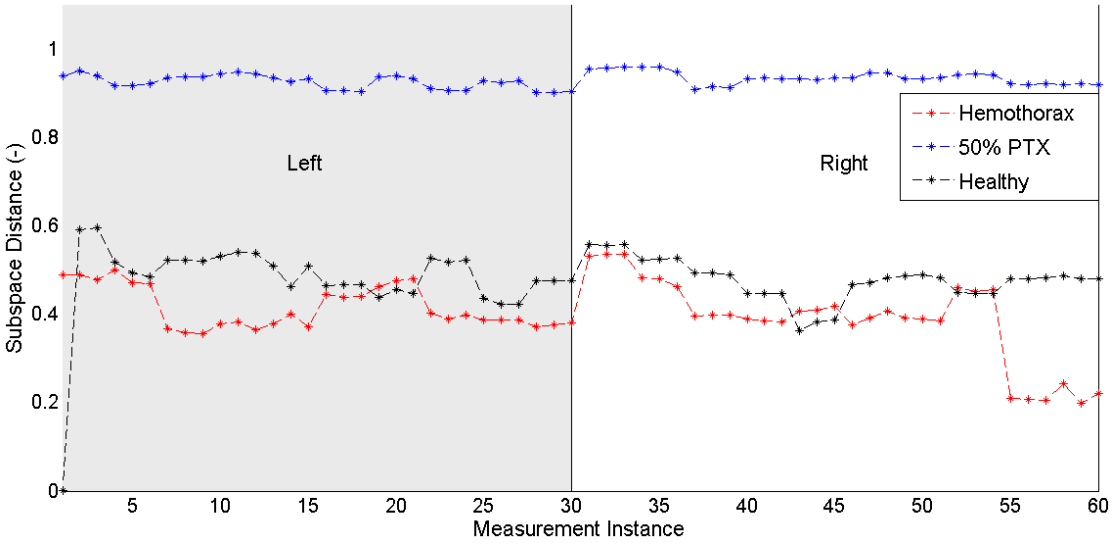

Figure 3.7: SVD subspaces distance of 50% PTX phantoms measurements, to subspaces of data gathered from 50% PTX phantoms, phantoms mimicking a healthy, and the hemothorax phantoms.

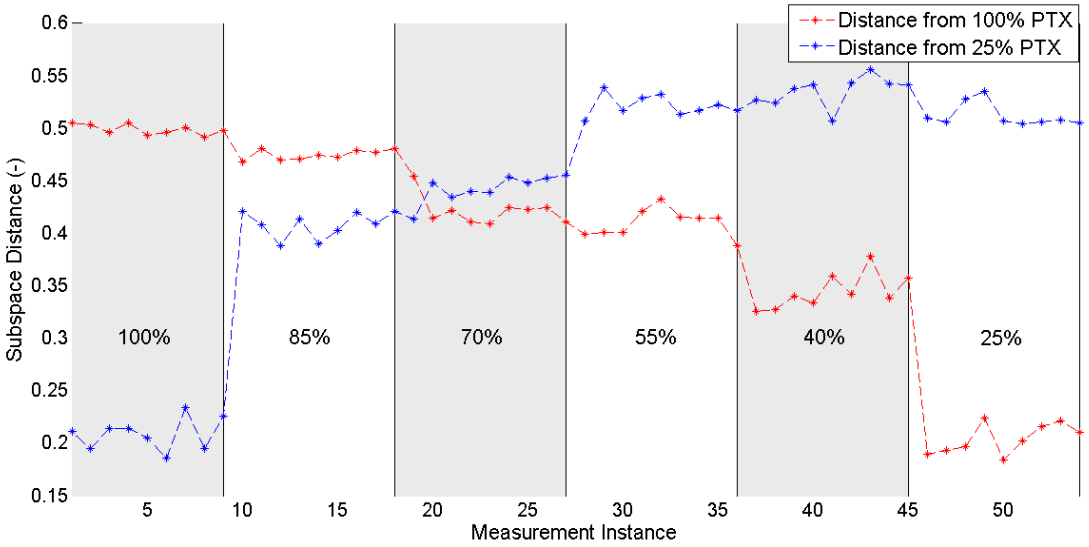

Figure 3.8: SVD subspace distance of data gathered from a phantom with decreasing PTX, to subspaces built using data from phantoms with a 100% PTX, and a 25% PTX.

4

Discussion

4.1 Performance of the developed thorax phantom and the measurement system

The first part of the work involved development of a thoracic phantom. It can be seen from a comparative analysis of the measurements made on the thoracic phantom, and measurements made on a a human test subject (Figure 3.3(a) and Figure 3.3(b)), that for antennas that were close to each other the attenuation profiles of the scattering parameters received correspond well to each other. But for antennas that were on different sides of the thorax, the signals travelling through a human subject was attenuated to a much larger extent than the signals that were measured from the phantom. This discrepancy most likely arises from the fact that there are various tissue interfaces present in the path between two antennas for the human body. These interfaces present a sharp change in dielectric properties which may cause scattering of the microwave signals and thus result in signal attenuation at the receiver. The environment in the phantom was homogeneous with only three major material interfaces(not considering the plastic of the cylinders themselves, as they do not effect microwave signals): thoracic tissue and lung, thoracic tissue and air, and air and lung tissue. Less tissue interfaces results in less scattering which implies that there is less signal attenuation. The phantom used was also slightly , than a human test subject (phantom circumference was 91.5 cm and for the human test subjects was 100 cm), thus offering more signal attenuation. Between the human subjects themselves, the signal attenuation profiles were similar to each other. But because of the high signal attenuation, for measurements made on biological specimens, it may become useful to analyse transmission and reflection coefficients measured by antennas on the same side only; the higher attenuation in the coupling between two contra-lateral antennas may adversely affect the quality

of information present in that signal but they may still provide useful insights into the state of the lungs. Moreover, the phantom used was is a static model. The thorax environment in a living human being is not static; a PTX grows larger and smaller in size with inspiration and expiration [28]. It is vital that the performance of this system be assessed in a dynamic environment.

The belt performed well in the test environment. The antennas could be placed consistently in the same position on the human test subjects and the thoracic phantoms. While making the measurements, the belt held the antennas securely in place. However the belt design is not perfect–it took two people to apply the belt correctly.

4.2 Data analysis

4.2.1 Fixed pneumothoraces

The classification of data gathered from phantom measurements gave mixed results. In Figure 3.5, data collected from phantoms which had pneumothoraces of different sizes (listed Table 3.1) . This was done by computing the SVD subspace distance of each measurement point (say m) in turn, to a SVD subspace built from data from phantoms without a PTX (phantoms mimicking a healthy patient), and a subspace of data from phantoms with a PTX (built without including the measurement point m). This analysis shows that there is a strong correlation between how similar the data sets collected from phantoms with or without a PTX were, and if the measurements were made on the same day, see Figure 3.5, and Table 3.1. Also, because of the nature of this analysis, the two subspaces made from PTX, and no PTX phantoms were not of the same size. The PTX phantoms' subspace had 177 data point and the non PTX phantoms' subspace had 60 data points. This can also influence classifier results.

4.2.2 Hemothorax

The same correlation, between measurement day and svd subspace distances, can be seen in hemothorax measurements also, Figure 3.6 and Figure 3.7. in Figure 3.6, it can be seen that measurement number 1 to 30 for phantoms mimicking a healthy patient, which were made on the same day as measurements number 1 to 30 on the phantoms with a 50% PTX, are very close to the SVD subspaces built from the data of phantoms mimicking a healthy patient. But for the last 30 50% PTX phantom measurements, the distance to the healthy subject phantoms' subspace is larger than it is for the first 30 measurements. In Figure 3.7, the same phenomena

is seen, where the subspace distances of the test phantoms' are found to be smaller to subspaces built using the measurements that were made on the same day as the test phantom, i.e., the data from phantoms mimicking a healthy subject. In other words, for the classifier used measurements being made on the same day is more significant criteria (for differentiating between measurement sets), than the differences in the construction of the phantoms themselves. This makes the difference in measurement day an undesirable signal artifact. Attempts to counteract this artifact through a recalibrating the PNA system before each measurement session, were not successful.

These results indicate that factors like measurement day, and instrument calibration can affect classifier results. In addition to this, the fact that, for practical reasons, an equal number of measurements were not made on phantoms with a PTX, a PTX and a hemothorax, and a phantom mimicking a healthy patient, means that there are additional biases in the classifier results.

4.2.3 Progressively decreasing pneumothorax

To account for uncertainties present in the previous measurement sets (measurements on phantoms with a pneumothorax of a fixed size and hemothorax), a set of measurements were made on a progressively decreasing PTX; keeping all experimental variable constant–these measurements were made on the same day, keeping the belt in the same position, and using the same instrument calibration. Figure 3.8 shows the classification results of measurements where the only difference between the upper baseline, the lower baseline, and the measurement from the PTX as it decreased in size, was the amount of air present in the right lung space, of each of the phantoms; all other experimental criteria were kept constant. An analysis of SVD subspace distances shows that as the PTX decreased in size, its subspace distance from the upper baseline increased and the distance from the lower baseline decreased. In other words, the fact that as PTX decreases in size it becomes more like a smaller PTX, and less like a larger PTX, is demonstrated in these results. This shows that in the absence of undesired measurement artifacts, the classifier can distinguish between phantoms using the amount of air present in the lung space as a measurement criteria.

4.3 Comparison with available diagnostic modalities

The primary diagnostic modalities for a PTX, i.e., CT, and AP X-ray, are only available at a hospital. It is for this reason that emergency medical technicians use the method of physical examinations to make an on–site diagnosis of a PTX, a technique that is fraught with problems of inaccuracy [7, 10]. To overcome

this challenge several new modalities for the diagnosis of a traumatic PTX have come up. Out of these two have emerged as front runners [9, 28]: ultrasounds, and the microwave based device, PneumoScan. The developed microwave based measurement instrumentation offers several advantages over the existing, and the upcoming modalities available to detect a PTX. Unlike an X-Ray or a CT unit, the measurement instrumentation is small enough to be installed in an ambulance, and is therefore more portable that those existing technologies. The microwave antenna array is an automated system, only requiring the application of belt onto the patient, by the operator. Once the belt is applied the system can make automated periodic measurements. The ability of the developed system to detect a progressively increasing pneumothorax can be employed here, to monitor a patience progress without the need of any intervention by a medical technician. The ultrasound, which requires a high level of operator competency with [30], and the PneumoScan [10], which uses a hand held probe which requires repeated application, do not offer this degree of simplicity, and automation in PTX detection. It is for these reasons that this technology merits further development.

5

Conclusions

Motivated by the fact that there is a need for an objective diagnostic tool for the detection of a traumatic pneumothorax caused by blunt trauma, the potential of microwave measurement based equipment was evaluated. The focus was to develop a device which would work in a situation outside the hospital conventional diagnostic tools are either unavailable or inaccurate. In the absence of human test subjects, measurements were made on a phantom of the human thorax, which served as a human analog. A singular value decomposition based classifier was then used to analyse the data from these measurements.

Conclusively, it can be said that from the results of the classifier analysis the potential of microwaves to detect a pneumothorax in a thoracic phantom has been demonstrated. Though the measurement technique used in this scientific work, suffers from artifacts introduced due to variations in measurement conditions: like the day of measurement, and instrument calibration. But in an ideal situation,i.e., for measurements made on the same day, using the same instrumentation calibration, there is a potential to detect and to even quantify the presence of air in a thorax phantom. The phantoms themselves were also shown to be a realistic approximation of the human thorax, albeit with some limitations; namely the fact that the phantom gave attenuation profiles dissimilar (for some antenna pairs) to those of measurements made on human test subjects. Also, in the phantom only a static environment was simulated.

6

Future Work

The results of the findings of this thesis work represent an analysis that is the first of its kind in several aspects. This is the first time a system which uses the changes in the thorax's dielectric properties, in the presence or absence of a simulated injury. Though phantoms used had some limitations. Future measurements can be made on phantoms that are a more accurate representation of a human thorax. Measurements can also be made on biological specimens, as they provide a test dynamic environment, e.g. porcine models that have been used to asses the utility of ultrasound to diagnose thoracic injuries[28]. In such a situation the measurement, and data analysis schemes can also be modified. Perhaps the measurements can be synchronised with the patient respiration, in such a way that all measurements are made when the thorax is at the same state of expansion. To take into account the differences in patient sizes the data analysis can be modified so that it compares the transmission and reflection coefficients of a patent's left and right lung. In the case of a unilateral PTX, such measurements may yield enough information to conclusively build a diagnosis

The developed microwave antenna array belt can also be modified to make it's use more convenient. In lieu of tying string at the back, Velcro straps can be incorporated into the belt. This will make belt application easier. The belt design can be further modified to be better suited for use in an ambulance or any other emergency care vehicle. In this scenario, evacuation boards are used to stabilise patients as they are moved from the sight of a trauma to a hospital. These boards have strapped built into them to secure the patient in place. Perhaps the microwaves antennas can be incorporated into these straps, to allow for quick and convenient application and removal.

Adding more antennas to each side, perhaps near the apex of the lung, near the second and third rib, merits consideration. However this must be weighed against the fact that more antennas increase system complexity, and the antennas themselves may restrict the access that a physician has to a patient being monitored by this system. Both of these scenarios are undesirable.

Bibliography

[1] S. Shackford, R. Mackersie, T. Holbrook, J. Davis, P. Hollingsworth-Fridlund, D. Hoyt, P. Wolf, The epidemiology of traumatic death. a population-based analysis, Archives of surgery (5) (1993) 571–575.

[2] K. Søreide, A. Krüger, A. Vårdal, C. Ellingsen, E. Søreide, H. Lossius, Epidemiology and contemporary patterns of trauma deaths: changing place, similar pace, older face, world journal of surgery (11) (2007) 2092–2103.

[3] T. Sundstrøm, S. Snorre, T. Wentzel-Larsen, K. Wester, Head injury mortality in the nordic countries, Journal Of Neurotrauma 24 (1) (2007) 147–153.
URL http://www.ncbi.nlm.nih.gov/pubmed/17263678

[4] Centers for Disease Control and Prevention, Cancer statistics by cancer type (2012).
URL http://www.cdc.gov/cancer/dcpc/data/types.htm

[5] A. Sharma, P. Jindal, Principles of diagnosis and management of traumatic pneumothorax, Journal of Emergencies, Trauma, and Shock 71 (1) (2008) 34–41.
URL http://www.ncbi.nlm.nih.gov/pmc/articles/PMC2700561/

[6] Al-Koudmani, et al., Chest trauma experience over eleven-year period at al-Mouassat University Teaching Hospital-Damascus: a retrospective review of 888 cases, Journal of Cardiotoracic Surgery 7.1 (1) (2012) 1–7.
URL http://www.cardiothoracicsurgery.org/content/7/1/35

[7] A. A. Ernst, W. A. M. McIntyre, S. J. M. Weiss, C. M. Berryman, Occult pneumothoraces in acute trauma patients, western Journal of Emergency Medicine 47 (5) (2012) 437–443.
URL http://escholarship.org/uc/uciem_westjem

[8] A. J. Blaivas, Collapsed Lung, Tech. rep., PubMed Health (July 2012).
URL http://www.ncbi.nlm.nih.gov/pubmedhealth/PMH0001151/

[9] D. Levy, P. Wielinski, T. Greszler, Micropower Impulse Radar: A Novel Technology for Rapid, Real-Time Detection of Pneumothorax, Emergency Medicine International Volume 1–5.

[10] M. Noppe, T. D. Keukeleire, Pneumothorax, Respiration 76 (2008) 121–127.
URL http://www.karger.com/Article/Pdf/135932

[11] R. C. Jacoby, F. D. Battistella, Hemothorax, Seminars in Respiratory and Critical Care Medicine 22 (6) (2001) 627–630.

[12] M. Kaiser, W. Matthew, B. Barrios, S. Dobson, D. Malinoski, M. Dolihch, M. Lekawa, D. Hyot, M. Cinat, The Clinical Significance of Occult Thoracic Injury in Blunt Trauma Patients, The American Surgeon 76 (10) (2010) 1063–1066.
URL http://www.ncbi.nlm.nih.gov/pubmed/21105610

[13] M. H. Baumann, M. Noppen, Pneumothorax, Respirology (9) (2004) 157–164.

[14] J. L. Heller, Pneumothorax - infants, Tech. rep., MedLinePlus (January 2012).
URL http://www.nlm.nih.gov/medlineplus/ency/article/007312.htm

[15] K. G. Bridges, G. Welch, M. Silver, M. A. Schinco, B. Esposito, {CT} detection of occult pneumothorax in multiple trauma patients, The Journal of Emergency Medicine 11 (2) (1993) 179 – 186.
URL http://www.sciencedirect.com/science/article/pii/073646799390517B

[16] J. Jones, F. Gaillard, Pulmonary Bleb, Tech. rep., Radiopaedia (March 2013).
URL http://radiopaedia.org/articles/pulmonary-bleb

[17] J. L. Heller, Hemothorax, Tech. rep., PubMed Health (October 2012).
URL http://www.ncbi.nlm.nih.gov/pubmedhealth/PMH0001183/

[18] M. A. Khorshidi, Classification of microwave scattering data with application to detection of bleeding stroke, Master's thesis, Chalmers Tekniska Högskola, ex - Institutionen för Signaler och System, Chalmers Tekniska Högskola, no: EX075/2009 (2009).
URL http://studentarbeten.chalmers.se/publication/99405-classification-of-microwave-scattering-data-with-application-to-detection-of-bleeding-stroke

[19] F. Farhang, H. Ting, Review of the use of microwave in investigating the dielectric properties of different human tissues 21 (2008) 679–682.
URL http://dx.doi.org/10.1007/978-3-540-69139-6_169

[20] M. A. Ahmad, Detecting traumatic intracranial bleedings in a brain phantom using microwave technology, ex - Department of signals and systems, Chalmers Technical University, no: EX042/2012 (2012).

[21] S. Krishnan, Microwave measurements on brain phantom for brain stroke diagnosis, ex - Department of signals and systems, Chalmers Technical University, no: EX103/2011 (2011).
URL http://studentarbeten.chalmers.se/publication/153304-microwave-measurements-on-brain-phantom-for-brain-stroke-diagnosis

[22] D. M. Pozar, Microwave engineering, 4th Edition, John Wiley Sons, Inc., 2011.

[23] C. Gabriel, S. Gabriel, E. Corthout, The dielectric properties of biological tissues: I. Literature survey, Physics in Medicine and Biology 41 (11) (1996) 2231–2249.
URL http://iopscience.iop.org/0031-9155/41/11/001

[24] D. M. Pozar, Microwave and RF Design of Wireless Systems, John Wiley Sons, Inc., 2001.

[25] S. Gabriel, R. Lau, C. Gabriel, The dielectric properties of biological tissues: II. Measurements in the frequency range 10 Hz to 20 GHz, Physics in Medicine and Biology 41 (11) (1996) 2251–2269.
URL http://iopscience.iop.org/0031-9155/41/11/002

[26] S. Gabriel, R. Lau, C. Gabriel, The dielectric properties of biological tissues: III. Parametric models for the dielectric spectrum of tissues, Physics in Medicine and Biology 41 (11) (1996) 2271–2293.
URL http://iopscience.iop.org/0031-9155/41/11/003

[27] T. Harrison, J. Wilson, Harrison's Principles of Internal Medicine, McGraw-Hill, 1991.

[28] N. P. Oveland, H. M. Lossius, K. Wemmelund, P. J. Stokkeland, L. Knudsen, E. Sloth, Using thoracic ultrasonography to accurately assess pneumothorax progression during positive pressure ventilation: A comparison with ct scanning, CHEST Journal 143 (2) (2013) 415–422.
URL http://dx.doi.org/10.1378/chest.12-1445

[29] M. Häggström, Tfile:naked human male body front anterior.png (Nov. 2008).
URL http://commons.wikimedia.org/wiki/File:Naked_human_male_body_front_anterior.png

[30] N. P. Oveland, E. Sloth, G. Andersen, H. M. Lossius, A porcine pneumothorax model for teaching ultrasound diagnostics, Academic Emergency Medicine 19 (5) (2012) 586–592.
URL http://www.ncbi.nlm.nih.gov/pmc/articles/PMC3502747/